Liquid Crystalline, Semifluorinated Side Group Block Copolymers with Stable Low Energy Surfaces: Synthesis, Liquid Crystalline Structure, and Critical Surface Tension

Jianguo Wang, Guoping Mao, Christopher K. Ober,* and Edward J. Kramer

Department of Materials Science and Engineering, Cornell University, Ithaca, New York 14853-1501

Received September 24, 1996; Revised Manuscript Received January 21, 1997[⊗]

ABSTRACT: Monodisperse poly(styrene-*b*-semifluorinated side chain) block copolymers were synthesized by anionic polymerization of poly(styrene-*b*-1,2/3,4-isoprene) followed by the corresponding polymer analogous reactions. By controlling the block copolymer composition and the relative lengths of the fluorocarbon and hydrocarbon units in the side group, the effect of chemical structure on surface properties and the influence of liquid crystalline structure of the semifluorinated side chain on the surface behavior were evaluated. The composition of side groups does not greatly affect the as-prepared sample surface tension, but influences instead the transition temperatures of the room temperature liquid crystal phase. It was observed that the shorter fluorocarbon units (six $-CF_2-$ units) form a smectic A phase at room temperature. The critical surface tension of the S_A phase is 10.8 mN/m, and the polymer surface undergoes significant reconstruction when immersed in water. However, when the fluorocarbon side chain contains more than eight $-CF_2-$ units, the resulting surface possesses a lower critical surface tension (ca. 8 mN/m) and exhibits negligible surface reconstruction. We believe the stability results from the highly ordered packing of the room temperature smectic B phase. This mesophase resists the reconstruction of the surface, since to do so would require loss of the enthalpies of transition. The estimated activation energy to destroy the smectic B phase is about 3−10 times higher than that of smectic A phase. This phase forms a uniform, hexagonally packed $-CF_3$ terminated surface with a low critical surface tension similar to that of fluorocarbon-based Langmuir−Blodgett films. The self-assembly of these liquid crystalline block copolymers at both the molecular and microstructural level provides a valuable approach to creating stable, low surface energy materials.

Introduction

In the development of low surface energy materials, it is a common approach to introduce a fluorinated group onto a polymer backbone in order to create a fluorinated surface coating.[1−6] Commercially available fluorinated ester side chain acrylic and methacrylic polymers are typical low surface energy coating materials.[1] As a result, fluorinated side chain block copolymers have potential applications as surface modifiers since a tiny amount of the fluorinated side chain block copolymer can be blended with the corresponding homopolymer to dramatically alter the surface properties of the blend. The surface segregation behavior of deuterium-labeled styrene-modified isoprene fluorinated side chain block copolymers in homopolystyrene blends has been well characterized by forward recoil spectrometry.[3,4] In these studies, the segregation isotherms at the air−polymer interface may be quantitatively described by a self-consistent mean field theory.[3,4] Chapman et al.[5,6] reported novel low surface energy fluorinated poly(amide urethane) block copolymers while Wynne et al. have examined other low surface energy polymers.[7,8] However, among these reported fluorinated block and segmented copolymers, one critical problem, surface reconstruction, still has not been resolved and limits the practical application of these block copolymers. The reason mainly attributed for this response is the poor stability of the amorphous fluorinated surface chains which cannot prevent movement of polar groups to the surface.

From a molecular level perspective, a uniformly organized array of trifluoromethyl ($-CF_3$) groups would be a surface with the lowest possible surface tension. Self-assembly of amphiphilic perfluorocarboxylic acid salts[9] occurs at the air−water interface of Langmuir−Blodgett (LB) films to produce among the lowest energy surfaces known. To prepare such a surface with LB film quality, trifluoromethyl groups must be aligned and oriented at the air−film interface. An effective alternative approach which avoids LB techniques for production of a uniform $-CF_3$ surface might be to harness the self-assembly behavior of a class of fluorinated materials, the liquid crystalline semifluorinated alkanes.

A high order smectic B mesophase has been previously identified in semifluorinated alkanes by Mahler et al.[10] in 1985 and was investigated in detail by Viney et al.[11,12] The same transition was regarded as a solid−solid transition by Rabolt.[13] Our studies on semifluorinated alkyl bromide compounds[14] supported the view that these compounds undergo a plastic crystal ("herring bone" layer structure) to smectic B transition before forming an isotropic melt. Although there is some disagreement about the correct mesophase structure of semifluorinated compounds, all investigations agree that the rigid-rod-like semifluorinated group can form a highly organized surface structure.

We have recently observed that a free-standing film of a semifluorinated side group ionene[15] possesses an extremely low critical surface tension (8 mN/m) due to its ability to arrange its fluorinated groups in a smectic layer structure. In these ionenes, the side groups are located in a highly ordered, liquid crystalline smectic B phase in which the $-CF_3$ end groups are arranged on the surface in a hexagonally organized layer. Semifluorinated groups have also been attached to siloxane-based polymers, and these elastomers also have low

[⊗] Abstract published in *Advance ACS Abstracts,* March 1, 1997.

S0024-9297(96)01412-X CCC: $14.00

surface energies.[16]

To be useful in practice as low energy surfaces not only must the low surface energy domains cover all of the surface but also all the side groups should be arranged in such a way as to avoid surface reconstruction. Although many fluorinated side groups have been introduced to block copolymers,[3−6] the effect of a liquid crystal (LC) structure such as a semifluorinated side group in a block copolymer is still unknown. From the above analysis, one might surmise that in order to prevent surface reconstruction processes from occurring it would be ideal that a side chain should also phase separate (i.e., have a long enough fluorocarbon unit to be immiscible with the polymer backbone and hydrocarbon side chain). Otherwise, the surface molecular composition would not be a uniform $-CF_3$ structure but would be a mixture of $-CH_3-$, $-CF_2-$, $-CH_2-$, and $-CH_3-$ groups. Bearing this idea in mind, self-organization at the size scales of a liquid crystalline mesogen could play an important role in the design of stable, low surface energy materials.

To achieve surface organization and enhance surface stability, we therefore introduced semifluorinated groups into a block copolymer to exploit their liquid crystalline properties. In this paper, a series of monodisperse polystyrene and semifluorinated alkane side group block copolymers (PS-*b*-P_{SFAS}) with various volume fractions of P_{SFAS} units and different lengths of fluorocarbon and hydrocarbon units in the side chains were synthesized as shown in Scheme 1. By systematically probing the effect of structure on the surface organization of the fluorocarbon side chain, study of these block copolymers has helped optimize the semifluorinated side groups for creating low surface energy materials. In addition, the interplay between the phase separation and liquid crystalline organization of the fluorinated block copolymers was also examined.

Experimental Section

Materials. Perfluorohexyl iodide (98%), perfluorooctyl iodide (97%), and perfluorodecyl iodide (97%) purchased from PCR Inc. were used without further purification. 3-Butene-1-ol (99%), 4-butene-1-ol (99%), 5-hexene-1-ol (99%), 9-decene-1-ol (98%), tributyltin hydride, nitrogen dioxide, and 0.5 M 9-borabicyclo[3.3.1]nonane (9-BBN) in tetrahydrofuran (THF) solution were used as received from Aldrich. A 30% hydrogen peroxide in water solution was used after purification by a freeze−thaw cycle to remove oxygen. Thionyl chloride was distilled from 10% triphenyl phosphite. Azoisobutyronitrile (AIBN, Merck) was recrystallized from acetone/methanol (1:1) at 0 °C. Poly(styrene-*b*-isoprene) polymers with 1,2- and 3,4-polyisoprene content greater than 97% were synthesized by living anionic polymerization.[17]

A typical synthetic procedure for the preparation of polystyrene−semifluorinated alkyl side group block copolymer is illustrated in Scheme 1. These polymers were prepared via classical living anionic polymerization followed by polymer analogous modification.

Hydroboration of Poly(styrene-*b*-isoprene). The block copolymers obtained from anionic polymerization had very narrow molecular weight distributions ($M_n/M_w < 1.1$) with the target block composition and microstructure. The 1,2- and 3,4-polyisoprene ratio was about 40/60 as determined by ^{1}H NMR. A detailed procedure for the anionic polymerization and hydroboration of poly(styrene-*b*-1,2- and 3,4-isoprene) was reported by Mao et al.[18] Work up of the hydroxylated block copolymer consisted of carefully precipitating the product into a 0.5−1.0 M KOH water/methanol solution to remove $NaB(OH)_4$ and dihydroxycyclooctane. The solvent mixture ratio of water to methanol depended on copolymer composition with polymers containing long hydroxylated blocks requiring more water. The solid product was filtered and dissolved in a methanol/tetrahydrofuran solution and reprecipitated three times. This procedural modification, (i.e., precipitating in base solution) was found to prevent effectively hydrolysis of $NaB(OH)_4$. This is important since residual $NaB(OH)_4$ hydrolyzed to boronic acid $B(OH)_3$ will cross-link the hydroxylated block copolymer. The product was dried overnight in a vacuum oven at 60 °C.

Scheme 1. Synthesis of Semifluroinated Block Copolymers

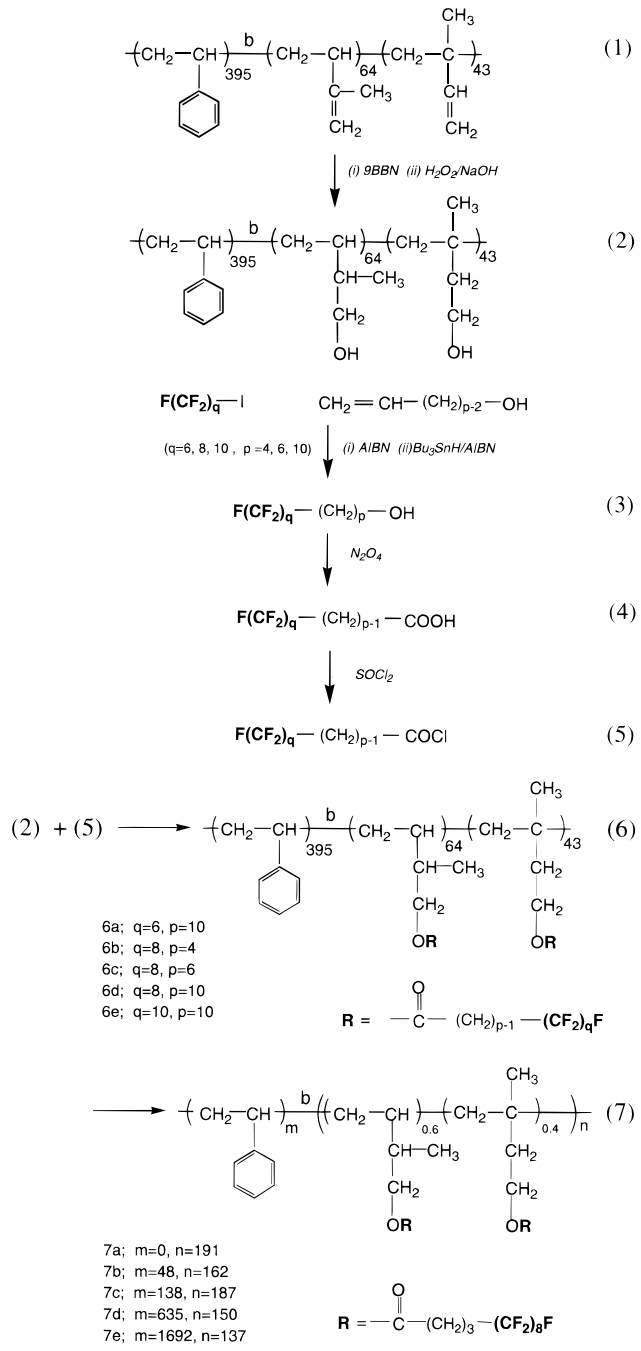

General Synthesis of Semifluorinated Acid Chloride. As shown in Scheme 1, the semifluorinated 1-alcohols **(3)** were synthesized by a known radical addition reaction[19] of perfluoroiodides to ω-alkene-1-ols. The alcohols were then oxidized with nitrogen dioxide. For example, 3.95 g (8.0 mmol) of **3b** $F(CF_2)_8(CH_2)_4OH$ was placed into a glass tube reactor (20 × 200 mm) equipped with a small magnetic stir bar, and sealed with a Teflon stopcock. At low temperature, ca. −40 °C, 1.9 g (40 mmol) of NO_2 was introduced into the reactor and slowly warmed to room temperature (18 °C). The stopcock was closed after the blue solid gradually turned brown, and the reaction was allowed to run at room temperature for 1 h, while the

solid white alcohol reacted and dissolved in the dark brown NO_2. The reactor was then slowly heated to 55 °C and held at this temperature for 48 h. After the reaction was cooled to room temperature, the stopcock was opened while excess nitrogen dioxide was removed by a vacuum aspirator. The white product was purified by sublimation at a temperature just below its melting point at 0.5 mmHg to yield 3.26 g of **4b** (yield 79%). The acid containing longer $-CF_2-$ ($q > 8$) acid could be recrystallized from dry diethyl ether.

4a: ^{1}H NMR ($CDCl_3$, δ in ppm) 2.34 (t, $J = 7.3$ Hz, -CH_2-COOH), 1.62 (2H, $-CH_2CH_2COOH$), 1.28 and 1.29 (10H, $(CH_2)_5CH_2CH_2COOH$), 1.58 (2H, $-CF_2CH_2CH_2-$), 2.03 (2H, $-CF_2CH_2$).

4b: ^{1}H NMR ($CDCl_3$, δ in ppm) 2.49 (t, 2H, $J = 7.0$Hz, $-CH_2COOH$), 1.95 (p, 2H, $J = 7.2$ Hz, $-CH_2CH_2CH_2-$), 2.17 (ttd, 2H, $-CF_2CH_2CH_2-$).

4c: ^{1}H NMR ($CDCl_3$, δ in ppm) 2.37 (t, 2H, $J = 7.2$ Hz, $-CH_2COOH$), 1.67 (2H, $-CH_2CH_2COOH$), 1.49 (2H, $-CF_2CH_2$-CH_2CH_2), 1.63 (2H, $-CF_2CH_2CH_2$), 2.05 (2H, $-CF_2CH_2$).

4d: ^{1}H NMR ($CDCl_3$, δ in ppm) 2.34 (t, $J = 7.3$Hz, $-CH_2$-COOH), 1.62 (2H, $-CH_2CH_2COOH$), 1.28 and 1.29 (10H, $(CH_2)_5CH_2CH_2COOH$), 1.58 (2H, $-CF_2CH_2CH_2-$), 2.03 (2H, $-CF_2CH_2$).

4e: same as **4d**.

The semifluorinated acid chlorides were prepared by reaction of the semifluorinated acids with thionyl chloride. As an example, 1.50 g (3 mmol) of solid **4b** containing 0.5 mL of $SOCl_2$ was added dropwise to a 10 mL round-bottomed flask. After proceeding at room temperature for 30 min, the reaction mixture was heated to 40 °C for 2 h, using vacuum to eliminate the excess $SOCl_2$ to yield ca. 1.32 g (yield 85%) of product **5b** after reduced pressure distillation.

Attachment reactions were carried out in a dry 5 mL flask, in which 300 mg of the hydroxylated block copolymer **2** (0.642 mmol of OH) was dissolved in 2 mL of anhydrous THF and 0.5 mL of pyridine. Then 420 mg (0.80 mmol) of 10% acid **5b**/THF solution was injected slowly through a rubber septum. During the reaction, white or slight yellow solid precipitated out (pyridine/hydrochloride salt). The reaction was maintained at 45 °C for another 10 h. Once the reaction was complete, 1 mL of anhydrous methanol was injected into the flask to convert the excess acid chloride to ester. The polymer solution was poured into copious amounts of a 1:1 methanol/water solution to remove excess semifluorinated ester and pyridine salt. The polymer was collected, dissolved in THF, and washed with water/methanol. This procedure was repeated five times before drying the polymer overnight at 60 °C in a vacuum oven.

Characterization. Proton and ^{19}F NMR spectra were obtained on a Varian 200 spectrometer at ^{1}H, 200 MHz, and ^{19}F, 188.2 MHz, while ^{13}C NMR was measured on a Varian FX-400 at 100.12 MHz. Deuterated chloroform was used as solvent. Chemical shifts were referenced to TMS for ^{1}H and ^{13}C NMR, and CF_3Cl for ^{19}F NMR. Infrared spectra were measured with a Mattson 2020 Galaxy series Fourier transform infrared spectrometer with 4 cm^{-1} resolution using 32 scans. Samples were pressed in a KBr tablet or cast on a NaCl crystal plate.

Gel permeation chromatography (GPC) was carried out using four Waters Styragel HT columns operating at 36 °C. The effective molecular weight range of the columns is from 500 to 10^7. GPC data was collected by a Waters 490 programmable multiwavelength detector. Molecular weights are quoted with respect to monodisperse polystyrene standards. THF was used as solvent and the GPC operated at 0.3 mL/min. Block copolymers were dissolved in THF at a concentration of 1.0 mg/mL. Polymer solution volumes of 20 μL were used for GPC measurement.

Differential scanning calorimeter (DSC) measurements were performed on a Perkin-Elmer DSC-7 Series instrument. Samples of 5−10 mg were used with a 10 °C/min heating rate and cooling rate. Nitrogen was used as purge gas at the flow rate of 30 mL/min. Polarizing optical microscopy was performed on a Nikon microscope with a Mettler FP 80 central processor hot stage and FX-35DX camera. Melting point, texture, and transition temperature were detected at heating rates of 1 °C/min.

Wide angle X-ray diffraction patterns were obtained by using a SCINTAG $\theta/2\theta$ diffractometer. The Ni-filtered Cu X-ray tube ($K\alpha = 1.5418$ Å) was operated at 45 kV and 40 mA. The temperature-dependent X-ray diffraction patterns were measured at the Cornell High Energy Synchrotron Source (CHESS).

Contact angles were determined using a NRC Contact Angle Goniometer Model 100-00 (Ramé-Hart Inc.) at 20 °C. Self-assembling films were prepared by slowly evaporating a 2% block copolymer/α,α,α-trifluorotoluene solution on a silica wafer at room temperature. The contact angles were averaged over four measurements. The advancing contact angle was read by injecting 4 μL liquid drops. The receding contact angle was measured by removing 3 μL of liquid from the droplet while the static contact angle was obtained using a free drop of liquid (ca. 4 μL) on the film surface. Linear alkanes and low molecular weight methyl terminated poly(dimethylsiloxane)s were used as standards to measure the critical surface tension.[20]

Results and Discussion

Synthesis. The synthesis and properties of semifluorinated alcohols were reported in detail in a separate paper.[15] Oxidation of the alcohol is very difficult to achieve by normal reagents such as CrO_3/H_2SO_4 (Jones agent) and K_2MnO_4 because of the very poor solubility of the semifluorinated compounds in water or organic solvents. Nitrogen dioxide has been reported to be an effective reagent for quantitative oxidation. The oxidation of normal aliphatic alcohol using N_2O_4 has been carried out at room temperature.[21] In our work, temperatures of ca. 50−60 °C, and longer reaction times (up to 2 days) in a closed system were necessary to completely convert the semifluorinated alcohols to acids as monitored by ^{1}H NMR. The acids were readily converted to acid chlorides and purified by reduced pressure distillation.

The base block copolymer was modified using a quantitative hydroboration reaction that was kept free from moisture and oxygen. The resulting product was precipitated in a basic solution in order to eliminate side reactions that might lead to crosslinking. GPC measurements indicated that monodispersity was retained after the hydroxylation reaction. The attachment of the semifluorinated side groups was carried out by formation of ester functions from the hydroxy groups and the semifluorinated acid chloride. The yield of the attachment reaction was close to 100% as discerned from FTIR and NMR measurements. The FTIR spectra exhibited no residual −OH groups after the esterfication reaction. Typical ^{13}C NMR spectra of the final block copolymer **6b** and their assignments are given in Figure 1. All the fluorocarbon side groups in the ^{13}C NMR spectra can be readily identified.

As listed in Table 1, 10 block copolymers were synthesized. Among them, polymers **6a**−**e** were prepared from the same polymer backbone with a degree of polymerization of the starting styrene and isoprene segments of 395 and 107, respectively. The polyisoprene block had 60% 1,2 and 40% 3,4 units as characterized by ^{1}H NMR. The only major difference in the resulting polymers was the nature of the fluorinated side chain as the volume fraction of all fluorinated segments was kept at approximately 50%−60%. The expected polymer morphology should therefore be in the lamellar region based on volume fraction. This approach was used to judge the influence of the side group as well as the liquid crystalline structure on the surface properties

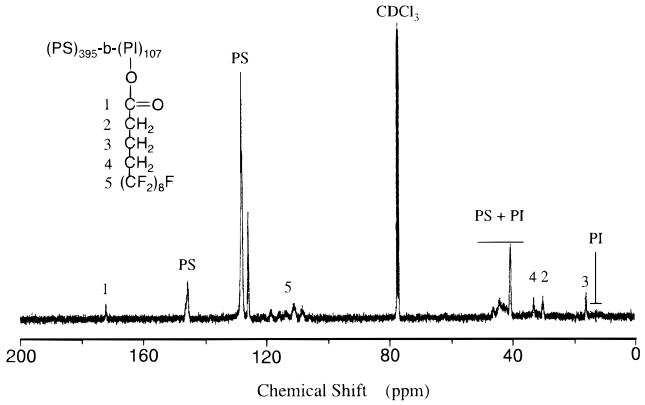

Figure 1. ^{13}C NMR spectrum of poly(styrene-*b*-semifluorinated side chain) block copolymer ($q = 8$, $p = 4$).

of the final blocks. Polymers **7a**−**e** were designed to have the same side chain (**5b)** but to alter the block ratio of the styrene and semifluorinated side group. Changing composition provides an avenue to explore the relationship between the morphology and surface properties.

Solution Properties of the Block Copolymers. The GPC measurements of the starting poly(styrene-*b*-isoprene), hydroxylated blocks, and semifluorinated alkyl side chain blocks are reported in Table 1. Generally, the polydispersity index of the block copolymers both before and after modification was less than 1.1. As shown in Table 1, the GPC-determined molecular weights of the hydroxylated and fluorinated polymers are lower than expected theoretically. The strong aggregation in THF solvent of either the hydroxylated or fluorinated blocks presumably leads to smaller hydrodynamic volumes relative to the base block copolymer.

Increased solution aggregation behavior of the semifluorinated side group block copolymers could be observed in polymers with larger perfluorocarbon units in the blocks. In Figure 2, two separate peaks appear in the GPC trace of **6d**. Both peaks are monodisperse ($M_w/M_n < 1.1$). The fraction of high molecular weight peaks diminished as the temperature was raised, and finally disappeared at temperatures above 60 °C. The semifluorinated side group homopolymer **6e** is almost insoluble in THF, and its GPC trace shows only very broad peaks at very short elution times. Therefore, the higher molecular weight peak was attributed to the formation of micelles in solution while the low molecular weight peak comes from isolated block copolymer molecules.

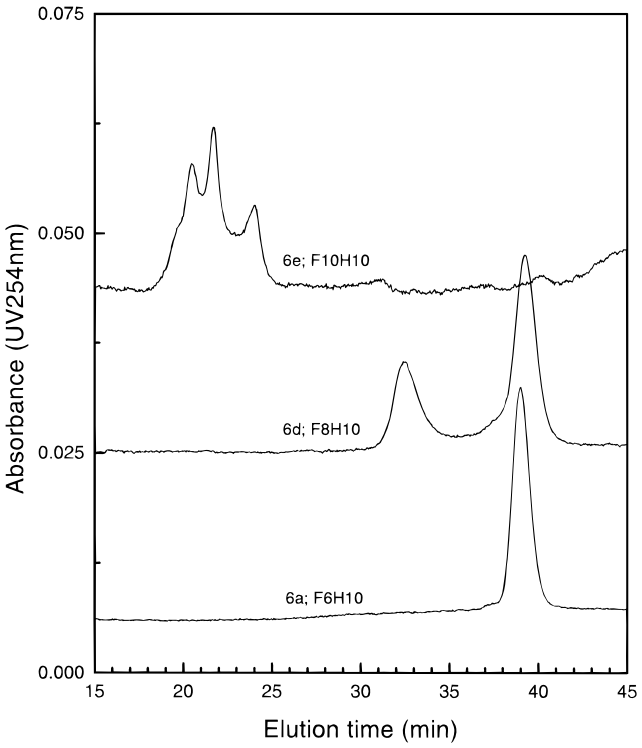

Figure 2. GPC traces of poly(styrene-*b*-semifluorinated side chain) block copolymers with different lengths of $-CF_2-$ units.

Figures 2 and 3 also show how the structure of the semifluorinated side chain will affect micelle formation by the block copolymer. Block copolymers **6a**−**e** have the same backbone but different side groups. Clearly, the longer the fluorocarbon unit in the side chain, the easier it is to form micelles in solution. Block copolymer **6a** with $-(CF_2)_6-$ units does not form micelles in THF solution. For the side chain with $-(CF_2)_8-$ groups at the same concentration, approximately 20% of the molecules form micelles as estimated from GPC peak area analysis, while almost 100% of the molecules form micelles for the 10 $-CF_2-$ side chain block. It is a well-understood phenomenon for block copolymers to form a micellar structure if one of the segments is insoluble in a given solvent.[22] Perfluorocarbon alkanes longer than six $-CF_2-$ groups are known[23] to be insoluble at room temperature in hydrocarbon solvents, while longer $-CF_2-$ alkanes are almost impossible to dissolve in any solvent. Therefore, the above results concerning the structure/micelle formation are consistent with the solubility of a fluorocarbon segment. A sufficiently long hydrocarbon spacer group will improve the solubility of

Table 1. GPC Characterization of Poly(styrene-*b*-semifluorinated side chain) Block Copolymers

		GPC results of starting PS/PI block		calculated results of final block of PS/PISF				
polymer	fluoro group[a]	M_n ratio	DP$_n$ ratio	M_n ratio	vol fraction of fluoro block	M_n (GPC[b])	polydispersity	micelle/free block ratio in THF from GPC[c]
6a	F6H10	41.1K/7.3K	395/107	41.1K/59.9K	55.4	82.7K	1.05	0/100
6b	F8H4	41.1K/7.3K	395/107	41.1K/61.6K	53.0	70.6K	1.07	20.7/79.3
6c	F8H6	41.1K/7.3K	395/107	41.1K/64.6K	54.9	71.4k	1.06	31/69
6d	F8H10	41.1K/7.3K	395/107	41.1K/70.6K	58.2	81.3K	1.08	72.3/27.7
6e	F10H10	41.1K/7.3K	395/107	41.1K/84.7K	61.4	*d*		100/0
7a	F8H4	0/13.0K	0/191	0/110K	100	*d*		
7b	F8H4	5.0K/11.0K	48/162	5.0K/93K	93.3	*d*		
7c	F8H4	14.4K/12.7K	138/187	14.4K/107K	84.8	*d*		
7d	F8H4	66.0K/10.2K	635/150	66.0K/86.3K	49.6	103K	1.07	19.8/80.2
7e	F8H4	176K/9.3K	1692/137	176K/78.7K	25.2	198K	1.10	100/0

[a] F*q*H*p* of semifluorinated 1-alcohol (see Scheme 1). [b] Polystyrene was used as standard for calculating molecular weight. [c] Calculated by relative intensity from UV-254 nm detector. [d] Polymer insoluble in THF.

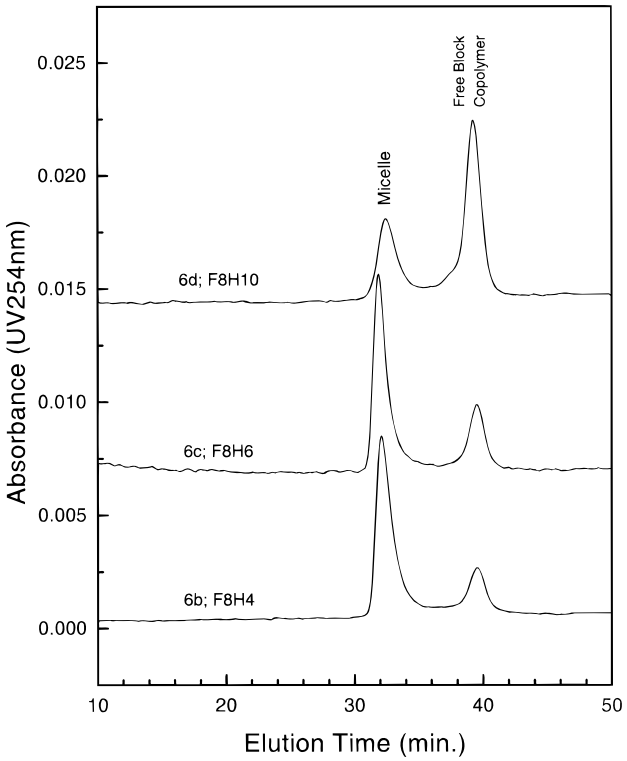

Figure 3. GPC traces of poly(styrene-*b*-semifluorinated side chain) block copolymers with different lengths of $-CH_2-$ units.

the side chain block and suppress the tendency of micelle construction. In Figure 3, only 20% of the **6d** $-(CH_2)_9-$ molecules form micelles; however, 30% of **6c** $-(CH_2)_5-$ and 80% of **6b** $-(CH_2)_3-$ form micelles. The aggregation number estimated from molecular weight is around 10. This uniform micelle structure may provide an interesting microreaction environment for the synthetic reaction of organofluorine compounds. Understanding the details of these block copolymer micelle structures is the subject of a future paper.

Thermal Studies of Semifluorinated Block Copolymers. The results of DSC measurements of the semifluorinated side group block copolymers are listed in Table 2. Typical DSC traces are also shown in Figure 4. In order to eliminate the effect of thermal history on sample transitions, all samples were heated to 160 °C (a temperature about 60 °C above the glass transition of the polystyrene block) and held at 160 °C for 1 min before cooling to −65 °C at a rate of 10 °C/min. The DSC data collected in the table were from the second run.

As illustrated in Table 2, two distinct first order transitions at temperatures T_1 and T_2 were observed in the block copolymers prior to the glass transition of

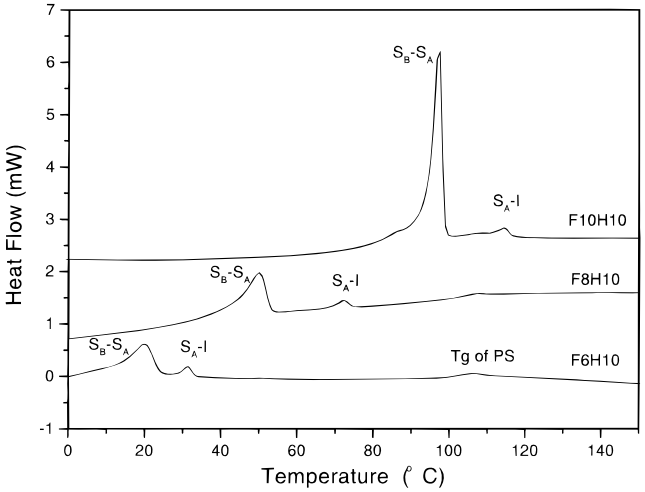

Figure 4. DSC traces of poly(styrene-*b*-semifluorinated side chain) block copolymers.

polystyrene. A DSC cooling run indicated that the above transitions were reversible. The lower transition temperature T_1 as well as the lower temperature transition enthalpy ΔH_{m1} are strongly dependent on the structure of the side group and increase with extension of both the $-CF_2-$ and $-CH_2-$ units. Thus, the lower temperature transition seems to be a structural change involving both segments of the side chain. As seen in Figure 4 (polymers **6a, 6d**, and **6e**) and Table 2, the higher temperature transition T_2 increased slightly with elongation of the $-CH_2-$ unit (from 61.0 °C for $-(CH_2)_3-$ to 72.2 °C for $-(CH_2)_9-$), but increased significantly with elongation of the $-CF_2-$ unit (from 31.3 °C for $-(CF_2)_6-$ to 114.4 °C for $-(CF_2)_{10}-$). However, the higher temperature transition enthalpy ΔH_{m2} is almost constant. These trends in melting behavior follow those of the semifluorinated parent compound,[14] such that the melting points are dominated by the $-CF_2-$ length and slightly affected by the $-CH_2-$ length. Thus, the low temperature transition seems to be a structural change involving both segments of the side chain. A detailed transition mechanism will be discussed in the section describing X-ray analysis.

Liquid crystalline side chain block copolymers have received growing attention in recent years[24−26] since these polymers can simultaneously organize on different length scales, thereby providing a new approach to tailoring material properties. Morphologies quite different than those expected from comparison to amorphous blocks of similar relative volume fraction have been reported.[27] At the same time, mesophase behavior has been affected. The semifluorinated alkyl side group is a unique type of phenyl-free rigid mesogen with a strong tendency to form a smectic phase. In addition,

Table 2. Thermodynamic Data of Polystyrene and Semifluorinated Side Chain Block Copolymers

polymer	side chain[a]	T_g of PS (°C)	T_1 (°C)	T_2 (°C)	ΔH_{m1}[b] (J/g)	ΔH_{m2}[b] (J/g)	loss of ΔH_m[c] (%)
6a	F6H10	100	19.9	31.3	7.4	1.0	
6b	F8H4	101	39.7	61.0	2.8	0.98	62.6
6c	F8H6	101	47.8	66.7	5.2	1.2	
6d	F8H10	101	49.9	72.2	10.3	0.94	
6e	F10H10	102	97.1	114.4	11.5	0.78	
7a	F8H4		52.6	69.8	4.6	5.5	0
7b	F8H4	99	51.1	67.9	4.0	4.6	14.9
7c	F8H4	101	47.6	67.2	2.3	2.9	48.5
7d	F8H4	101	35.3	56.2	1.1	1.4	75.3
7e	F8H4	102		48.2		~0.2	98

[a] F*q*H*p* of semifluorinated 1-alcohol (see Scheme 1). [b] Calculated as per gram semifluorinated side chain. [c] Normalized by homopolymer **7a**.

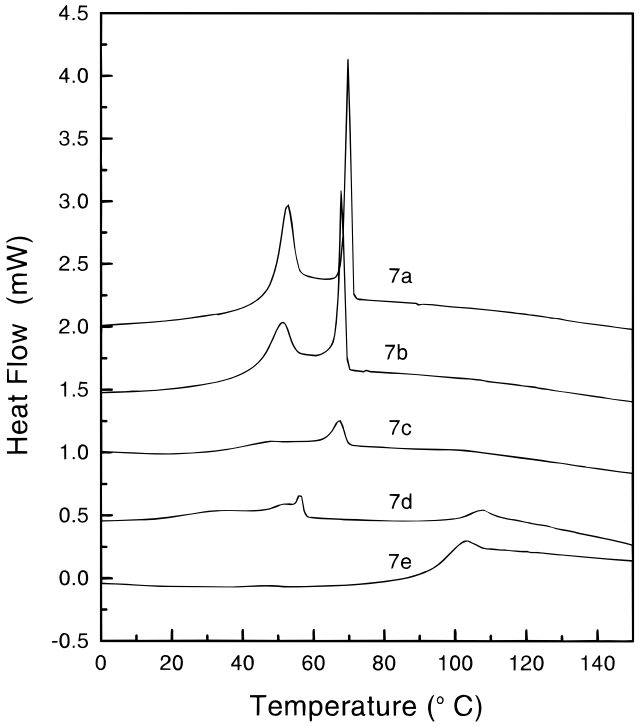

Figure 5. DSC heating run of block copolymers with different compositions.

the fluorinated mesogenic group is an intrinsic low surface energy element. In comparison to LC-coil block copolymers with conventional side group mesogens, semifluorinated side chain block copolymers exhibit a more pronounced ability to organize in both organic solution and the solid state,[28] as a result of their low surface energy character and strong phase separation.

It has been reported that the incorporation of mesogenic groups into a block copolymer can have a profound effect on transition amplitude and phase behavior depending on the domain type and size in LC-coil block copolymers.[25] In order to examine the liquid crystal behavior of semifluorinated side groups in block copolymers, the transition temperatures and enthalpies of LC-coil block copolymers of different relative lengths were measured by DSC. These results are listed in Table 2 and are shown in Figure 5. The low fluorocarbon content block copolymers such as **7d** exhibited particularly low transition temperatures and enthalpies compared to the semifluorinated side group homopolymer, **7a**. A lower fluorine content block copolymer such as **7e** with ca. 25% vol fraction semifluorinated component has a clearing transition (temperature T_2) that is so small it is difficult to detect. As the volume fraction of the side group decreases, the enthalpy reduction grows from 15% to 98%. This can be interpreted as an increasing influence on the mesophase by the interface between the semifluorinated and polystyrene domains. Obviously, the semifluorinated segment will change from forming a continuous phase to being the dispersed phase with a decrease in block content. The organization of the smectic liquid crystalline layer into spherical domains in the dispersed phase will be difficult due to the small radius of curvature of the interfaces.

X-ray Studies of the Block Copolymers. Results of room temperature (18 °C) powder X-ray diffraction measurements on the block copolymers are listed in Table 3. At room temperature all the block copolymers exhibited diffraction peaks of 4.8−5.0 Å with some additional strong diffraction peaks in the small-angle

Table 3. X-ray Diffraction Data of Poly(styrene-*b*-semifluorinated side chain) Block Copolymers

polymer	fluoro group[a]	molar composition (PS/PISF)	*d* spacing[b] (Å)
6a	F6H10	84.9/15.1	33.8 (s), 17.0 (vw), 4.84 (very broad)
6b	F8H4	84.9/15.1	32.2 (s), 16.2 (m), 10.7 (w), 5.06 (broad)
6c	F8H6	84.9/15.1	35.2 (s), 17.6 (w), 11.7 (m), 4.95 (broad)
6d	F8H10	84.9/15.1	40.1 (s), 13.4 (w), 4.83 (broad)
6e	F10H10	84.9/15.1	46.3 (vs), 15.7 (s), 4.85 (sharp)
7a	F8H4	100/0	34.3 (vs), 16.8 (s), 11.42 (m), 4.93 (sharp)
7b	F8H4	77.1/22.9	33.7 (s), 16.7 (m), 11.23 (w), 4.979 (sharp)
7c	F8H4	57.4/42.6	33.9 (s), 16.7 (w), 11.11 (w), 4.98 (broad)
7d	F8H4	19.1/80.9	32.3 (s), 16.0 (w), 10.74 (w), 5.01 (broad)
7e	F8H4	7.5/92.5	∼36 (w)

[a] F*q*H*p* of semifluorinated 1-alcohol (see Scheme 1). [b] vs, very strong; s, strong; m, medium; w, weak; vw, very weak.

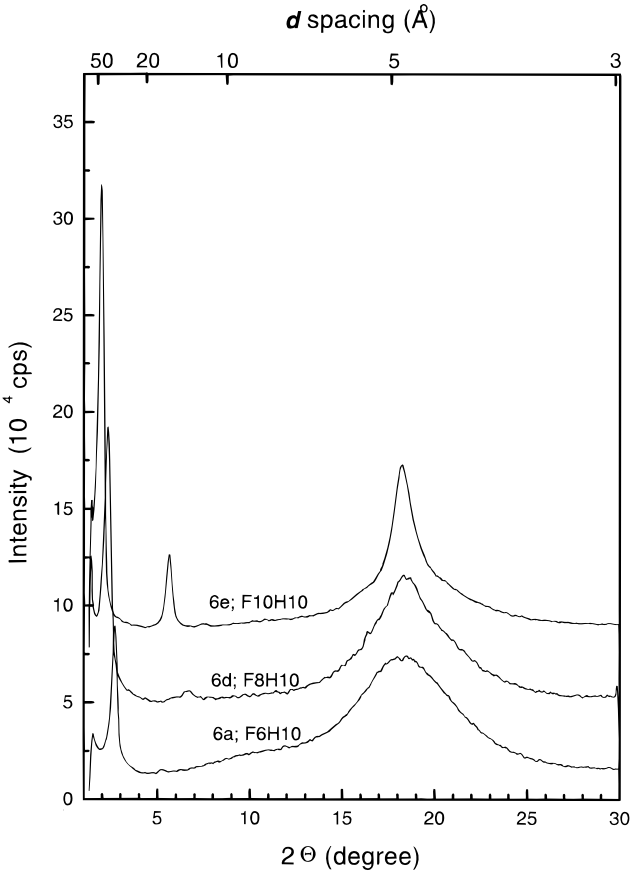

Figure 6. X-ray diffraction plots of poly(styrene-*b*-semifluorinated side chain) block copolymers.

region due to the mesogenic group layering. However, as illustrated in Figure 6, block copolymer **6a** $-(CF_2)_6-$ had much broader peaks at 5.0 Å than polymer **6d** $-(CF_2)_8-$ or **6e** $-(CF_2)_{10}-$. The diffraction peak at 5 Å is the intermolecular spacing of the cylindrical perfluorocarbon molecules arranged in a hexagonally packed layer. The layer distance in the small angle region of **6a** is close to that calculated from the molecular length of semifluorinated segments organized in a head-to-head arrangement. The X-ray fiber patterns of **6a** indicate that the small angle diffraction peak is perpendicular

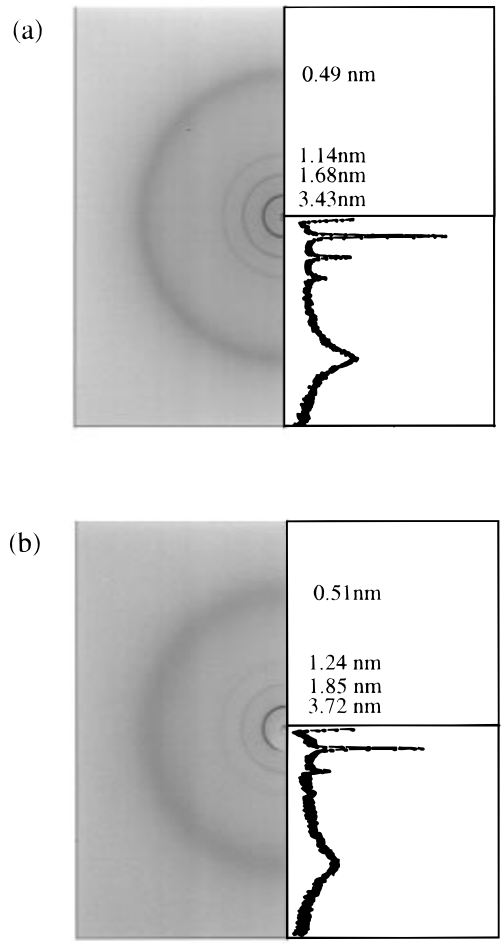

Figure 7. X-ray patterns of semifluorinated side chain homopolymer: (a) at 25 °C (smectic B phase); (b) at 60 °C (smectic A phase).

Table 4. Water Contact Angles and Critical Surface Tension of Poly(styrene-*b*-semifluorinated side chain) Block Copolymers

polymer	composition (PS-*b*-PISF)	fluoro group[a]	H_2O contact angle		critical surface tension (mN/m)
			Advancing	Receding	
6a	41.1K/59.9K	F6H10	111	86	10.8
6b	41.1K/61.6K	F8H4	120	109	8.5
6c	41.1K/64.6K	F8H6	120	108	8.5
6d	41.1K/70.6K	F8H10	122	110	8.2
6e	41.1K/84.7K	F10H10	123	112	8.0
7a	0/110K	F8H4	121	111	8.1
7b	5.0K/93K	F8H4	120	109	8.3
7c	14.4K/107K	F8H4	120	109	8.5
7d	66.0K/86.3K	D8H4	118	107	8.5
7e	176K/78.7K	F8H4	108	95	9.9

[a] F*q*H*p* of semifluorinated 1-alcohol (see Scheme 1).

to the wide-angle 5.0 Å diffraction peak; i.e., if the 5.0 Å peak lies on the equator of the patterns, the small angle peak lies alongs the meridian. Both the spacing and orientation permit the assignment of the mesophase of the semifluorinated block copolymer **6a** at room temperature to a lower order smectic A phase which corresponds to the state before the high temperature transition. For the long semifluorinated side chain, $q > 6$, as illustrated in Figure 7, the sharp wide angle diffraction ring is more obvious in the semifluorinated side chain homopolymer **7a** due to the absence of the diffuse polystyrene scattering ring. At the temperature just above the first transition (60 °C), as detected from

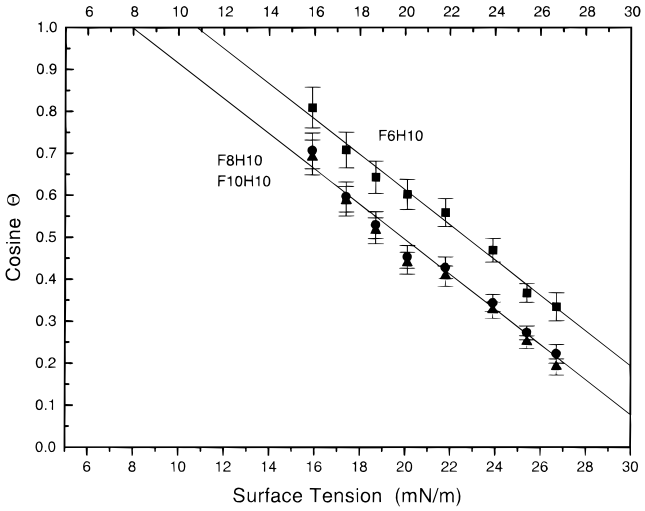

Figure 8. Zisman plot of poly(styrene-*b*-semifluorinated side chain) block copolymers.

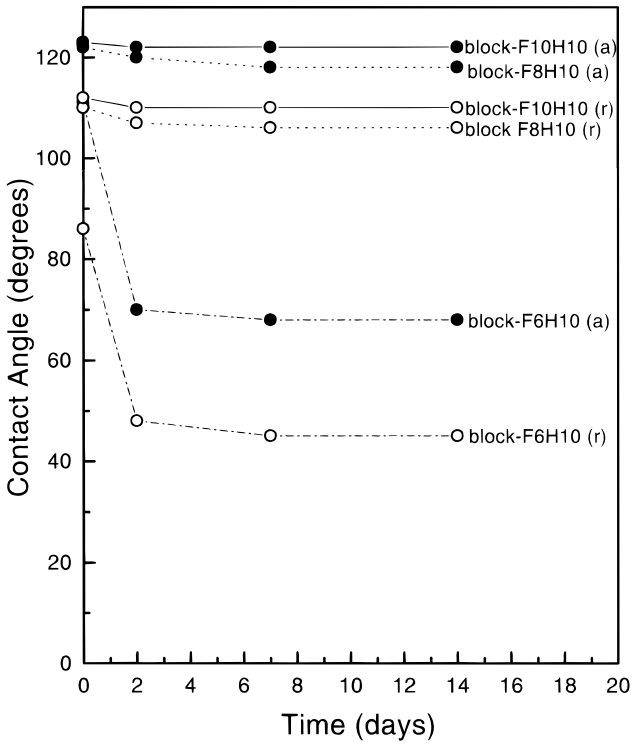

Figure 9. Time-dependent advancing (a) and receding (r) water contact angles of different semifluorinated side chain polymer films.

DSC traces (Figure 4), the wide angle ring becomes much broader and weaker similar to the room temperature small angle diffraction ring of **6a**, while the smectic layer spacing decreases about 2−3 Å compared to the room temperature spacing. An oriented fiber pattern shows that the mesogen is oriented in the same direction as **6a** during the entire transition; thus the low temperature phase can be identified as smectic B. Detailed structural characterization including the microstructure and mesophase will be reported in a separate paper.

From the DSC and X-ray analysis above, we find that the semifluorinated alkane side chains have two mesophases. Below the low temperature transition, side chains are arranged in a high order head-to-head bilayer smectic B phase. Upon heating, the hexagonal symmetry between the semifluorinated segments is lost, and

Scheme 2. Schematic Representation of the Relationship between the Semifluorinated Side Chain End Structures and Their Critical Surface Tensions

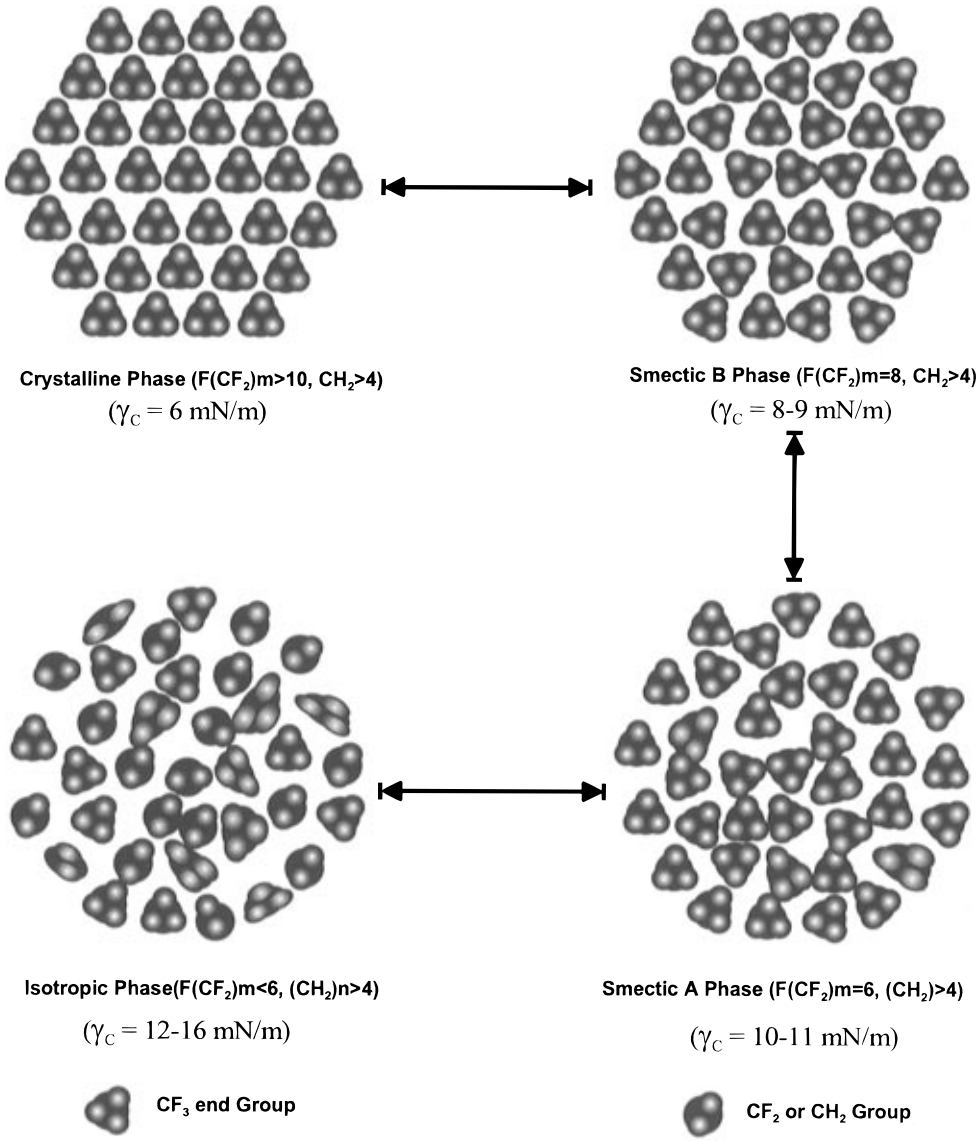

a low order smectic A phase could be observed. Compared to the low molar mass semifluorinated alkanes,[10−14] the smectic A phase in the polymer is an additional phase which occurs between the smectic B and isotropic phase. One possible interpretation is that the polymer backbone fixes the tail of the semifluorinated side chain and stabilizes the smectic A phase.

Surface Tension Studies of Semifluorinated Side Chain Blocks. As an important measure of the hydrophobic properties of the surface, water contact angles were evaluated and are listed in Table 4. The critical surface tensions extrapolated from Zisman plots are also included. The advancing contact angle for most of these block copolymers was only about 10° higher than the receding contact angle, making the contact angle hysteresis of the films much smaller than that reported for many low energy surfaces.[6−8] A simple explanation is that the fluorinated groups of the block copolymers reside in a mesophase at room temperature. This mesophase resists the reconstruction of the surface since to do so would require loss of the enthalpies of transition ΔH_1 and ΔH_2. Figure 8 shows a typical Zisman plot of block copolymers **6c**, **6d**, and **6e** in contact with a series of hydrocarbon and silicone oils.

Considering the different molecular and liquid crystal structures of the block copolymers and their critical surface tensions listed in Table 4, some useful conclusions can be deduced. For the same block copolymer, longer fluorocarbon side chains will produce a lower surface tension. The water contact angle of **6d** $-(CF_2)_{10}-$ is about 12° higher than that of **6a** $-(CF_2)_6-$. On the basis of a structural analysis, one can suggest that the longer fluorocarbon side chains produce a higher order smectic B layer on the surface while shorter side chains form a smectic A layer though both have a strong tendency to segregate to the surface. Consequently, the smectic B surface will construct a uniform hexagonal close packed array of perfluorocarbon side chains and present a regular CF_3 surface. Such a surface is indicated by the low value of critical surface tension (8.0 mN/m) obtained for **6e**, which is very close to that for a LB film surface of the corresponding perfluorocarbon acid. Approximately eight $-(CF_2)-$ units provide the optimal length for the perfluorocarbon units to self-assemble into a low energy surface for room temperature applications because longer $-CF_2-$ chains are insoluble in conventional solvents at room temperature. On the other hand, $-CH_2-$ spacer groups do not have

a large effect on the surface tension, but longer $-CH_2-$ spacer groups render the side chain packing more stable (higher S_B-S_A transition temperature and higher transition enthalpy) and the polymer becomes more soluble. Therefore, a spacer of 8−10 CH_2 groups is a suitable length for creating a low surface energy material. The copolymer morphology has little effect on surface tension if the fluorinated segment is a continuous phase. Surface tension clearly decreases with the concurrent transition enthalpy loss and lowering of the transition temperature if the volume fraction decreases below 20% since then it is difficult to form a stable smectic layer at the surface.

In order to examine the surface stability of the films, long-term contact angle measurements were carried out after immersion of the films into water for 2 weeks at 22 °C. As seen in Figure 9, the advancing contact angle of water-soaked block copolymer **6d** decreases by 2−3° relative to the same, unsoaked block copolymer film while **6e** was almost the same as the unsoaked film. In this case, water can still be readily removed from the surface even after immersion in water for 2 weeks. However, the advancing contact angle of **6a** dropped to 70°, about 40° lower than that of the original film. One reasonable explanation of this difference is that the smectic A phase (i.e., the surface of **6a**) has a much lower (by a factor of 0.3 to 0.1) transition enthalpy to disordered isotropic state than does the smectic B phase (i.e., the surface of either **6d** or **6e**). The smectic A surface in contact with water can reconstruct to expose the more polar ester linkage by reorientation of a few semifluorinated groups at a time without paying a relatively high enthalpy penalty. The smectic B surface in contact with water must pay a much larger enthalpy penalty for such reconstruction. The smectic B surface is thus much more stable in contact with water. Our mental picture of the structures of the various surfaces are shown schematically in Scheme 2, where the trifluoromethyl end group structure changes from crystal to liquid crystal to disordered amorphous phase as the film is heated. The apparent connection between bulk mesophase and surface stability suggests that tailoring of the surface may be controlled by proper selection of the LC phase of the surface-forming component.

Conclusions

In summary, while designing low surface energy materials, a family of monodisperse polystyrene−semifluorinated alkyl ester side chain block copolymers were synthesized by polymer analogous reactions on poly(styrene-*b*-1,2/3,4- isoprene) block copolymers. Varying lengths of perfluorocarbon and hydrocarbon units in the side chain give rise to different liquid crystalline phases, which affect such surface properties as the critical surface tension and surface stability. Semifluorinated side chains with less than six $-CF_2-$ segments form smectic A phases at room temperature from which $-CF_3$ moieties are exposed to the surface by surface segregation. The surface tension of a S_A surface was measured as 10.8 mN/m which shows surface reconstruction after long-term water exposure by contact angle measurements. In contrast, semifluorinated side chains with more than six $-CF_2-$ units form high order smectic B or plastic crystal structures from which nearly uniform hexagonal close packed $-CF_3$ surfaces are produced. The critical surface tension is 8 mN/m without noticeable surface reconstruction in water. The longer hydrocarbon spacer groups not only improve the solubility of fluorinated materials but also enhance their thermal stability. The relative volume fraction of the block copolymers (composition of blocks) does not influence critical surface tension, but significantly affects the thermal stability of the LC phase as confirmed from the major loss of transition enthalpy at small fluorinated block volume fractions. These block copolymers also form small monodisperse micelles in normal organic solvents.

Acknowledgment. This research was supported by the Office of Naval Research, Grant No. N00014-92-J-1246. The ^{13}C NMR spectra measured by Mr. S. C. Clingman are appreciated. G.M. thanks the National Science Foundation for financial support. Dr. H. Körner and A. Shiota provided invaluable help with the X-ray diffraction measurements. The use of the MSC facilities and the Cornell High Energy Synchrotron Source (CHESS) is acknowledged.

References and Notes

(1) Pittman, A. G. In *Fluoropolymers*; Wall, L.A., Ed.; Wiley: New York, 1972; Vol. 25, p 419.
(2) Schmidt, D. L.; Coburn, C. E.; Dekoven, B. M.; Potter, G. E.; Meyers, G. F.; Fisher, D. A. *Nature* **1994**, *368*, 39−41.
(3) Hwang, S. S.; Ober, C. K.; Perutz, S.; Iyengar, D.; Schneggenburger, L. A.; Kramer, E. J. *Polymer* **1995**, *36*, 1321−1324.
(4) Iyengar, D. R.; Perutz, S. M.; Dai, C.-A.; Ober, C. K.; Kramer, E. J. *Macromolecules* **1996**, *29*, 1229−1234.
(5) Chapman, T. M.; Benrashid, R.; Marra, K. G.; Keener, J. P. *Macromolecules* **1995**, *28*, 331−335.
(6) Chapman, T. M.; Marra, K. G. *Macromolecules* **1995**, *28*, 2081−2085.
(7) Wynne, K. J.; Ho, T.; Vu, A.; Chen, X.; Gardella, Joseph, A. Jr. *Polym. Prepr.* (*Am. Chem. Soc., Div. Polym. Chem.*) **1995**, *36* (1), 67−68.
(8) Pike, J. K.; Ho, T.; Wynne, K. J. *Chem. Mater.* **1996**, *8*, 856−860.
(9) Bernett, M. K.; Zisman, W. A. *J. Phys. Chem.* **1960**, *64*, 1292.
(10) Mahler, W.; Guillon, D.; Skoulios, A. *Mol. Cryst. Liq. Cryst. Lett.* **1985**, *2*, 111.
(11) Viney, C.; Russell, T. P.; Depero, L. E.; Twieg, R. J. *Mol. Cryst. Liq. Cryst.* **1989**, *168*, 63.
(12) Viney, C.; Twieg, R. J.; Russell, T. P.; Depero, L. E. *Liq. Cryst.* **1989**, *5*, 1783.
(13) Russell, T. P.; Rabolt, J. F.;Twieg, R. J.; Siemens, R. L. *Macromolecules* **1986**, *19*, 1135.
(14) Ober, C. K.; Wang, J. G.; Mao, G. P. *Abstract of 35 IUPAC Macromolecules*, Soel, August 1996, in press.
(15) Wang, J. G.; Ober, C. K. Kramer, E. J. *Polym. Prepr.* (*Am. Chem. Soc., Div. Polym. Chem.*) **1996**, *37* (2), 815.
(16) Perutz, S. M.; Wang, J. G.; Ober, C. K.; Kramer, E. J. *Polym. Prepr.* (*Am. Chem. Soc., Div. Polym. Chem.*) **1996**, *37* (2), 45.
(17) Mao, G. P; Wang, J. G.; Clingman S. R.; Ober, C. K. *Macromolecules*, in press.
(18) Mao, G. P.; Clingman, S. R.; Ober, C. K.; Long, T. E. *Polym. Prepr.* (*Am. Chem. Soc., Div. Polym. Chem.*) **1993**, *34* (2), 710.
(19) Höpken, J.; Möller, M.; Boileau, S. *New Polym. Mater.* **1991**, *2*, 339.
(20) Zisman, W. A. In *Contact angle, wettability, and adhesion*; American Chemical Society: Washington, DC, 1964.
(21) Langenbeck, W.; Richter, M. *Chem. Ber.* **1956**, *89*, 202.
(22) Tuzar, Z.; Kratochvil, P. *Surf. Colloid Sci.* **1993**, *15*, 1.
(23) Bedford, R. G.; Dunlap, R. D. *J. Am. Chem. Soc.* **1958**, *80*, 282.
(24) Adams, J.; Gronski, W. *Makromol. Chem., Rapid Commun.* **1989**, *10*, 553.
(25) Bohnert, R.; Finkelmann, H. *Macromol. Chem. Phys.* **1994**, *195*, 689.
(26) Yamada, M.; Iguchi, T.; Hirao, A.; Nakahama, S.; Watanabe, J. *Macromolecules* **1995**, *28*, 50.
(27) Fisher, H.; Poser, S.; Arnold, M.; Frank, W. *Macromolecules* **1994**, *27*, 7133.
(28) Ober, C. K.; Wang, J. G.; Mao, G. P.; Kramer, E. J.; Thomas, E. L. *Macromol. Chem., Macromol. Symp.*, in press.

MA961412O